



# Study of the process $e^+e^- \rightarrow \pi^+\pi^-\pi^0\eta$ with the CMD-3 detector on VEPP-2000

P. Basova E. Solodov

Budker Institute of Nuclear Physics, Novosibirsk



## Abstract

The analysis of the process  $e^+e^- \rightarrow \pi^+\pi^-\pi^0\eta$  uses data collected by the CMD-3 detector at the VEPP-2000 accelerator during the 2019-2023 years, corresponding to an integrated luminosity of  $481.7 \text{ pb}^{-1}$  in the center-of-mass energy range of 1440 - 2007 MeV. The preliminary cross section of the process  $e^+e^- \rightarrow \pi^+\pi^-\pi^0\eta$  and the contributions from intermediate resonant states  $\omega(782)\eta$ ,  $\phi(1020)\eta$  and  $a_0(980)\rho(770)$  were measured. The current status of the analysis is presented.

## VEPP-2000 and CMD-3

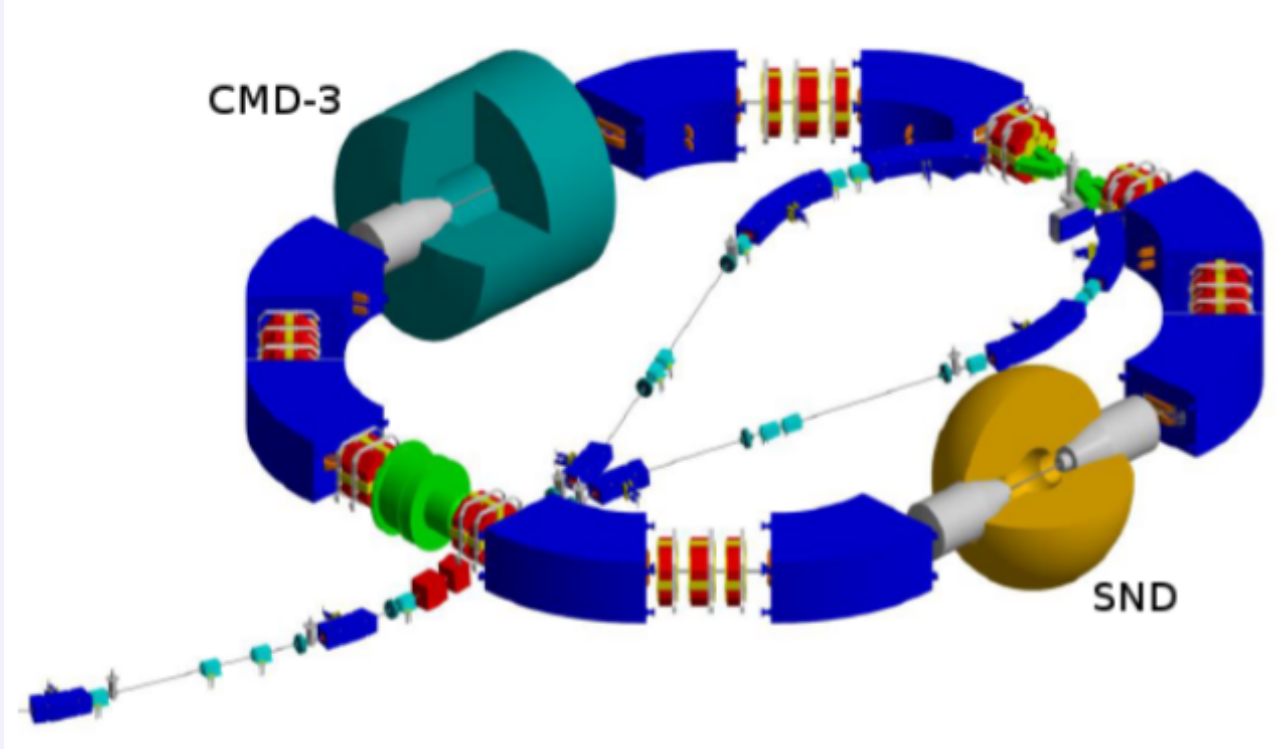


Figure 1. Scheme of the VEPP-2000.

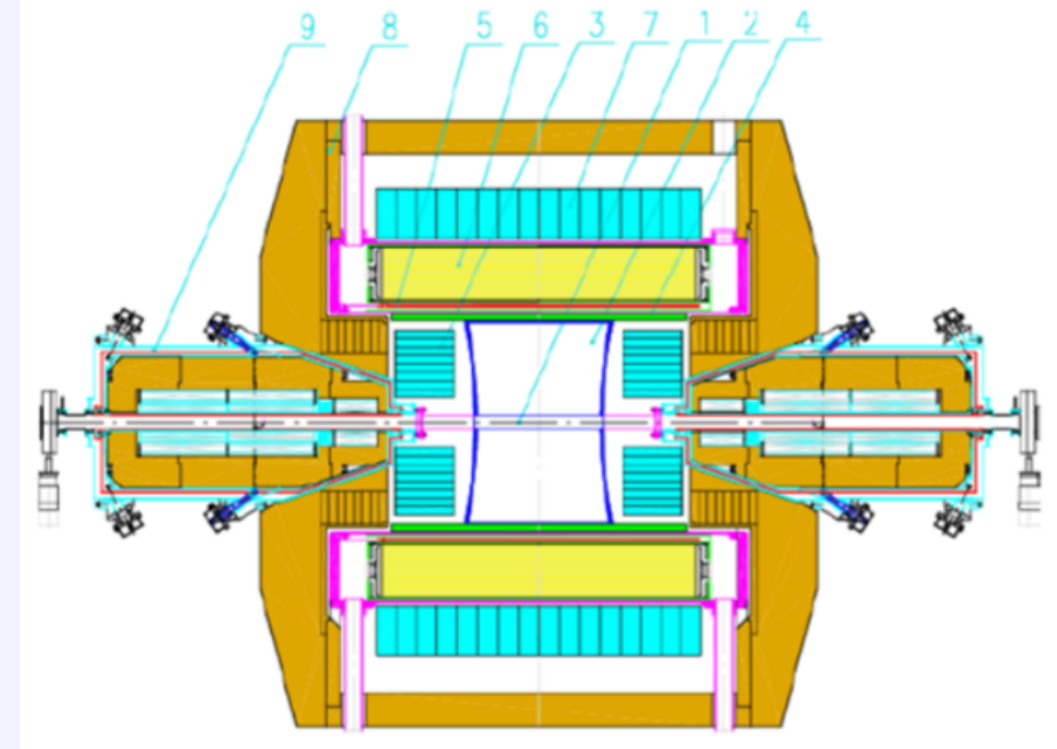


Figure 2. Scheme of the CMD-3 detector.

- round beam optics
- beam current – 0.2 A
- beam length – 3.3 cm
- beam energy spread – 0.7 MeV
- $L = 10^{32} \text{ cm}^{-2} \text{ s}^{-1}$  at  $2E=2.0 \text{ GeV}$
- $L = 2 \cdot 10^{31} \text{ cm}^{-2} \text{ s}^{-1}$  at  $2E=1.0 \text{ GeV}$

1. vacuum chamber,
2. drift chamber,
3. BGO-calorimeter,
4. Z-chamber,
5. superconducting solenoid,
6. LXe-calorimeter,
7. CsI-calorimeter,
8. yoke,
9. solenoid of VEPP-2000.

## Selection criteria

- **Good tracks**  $\pi^+\pi^-$ 
  - Opposite charges
  - Noncollinearity  $|\phi_1 - \phi_2| - \pi < 0.15$  and  $|\Theta_1 + \Theta_2| - \pi < 0.25$
  - Momentum  $p$  is greater than 40 MeV/c and less than the beam energy
  - Number of hits is greater than 5
  - Vertex in the beam interaction region: impact parameter  $|\rho| < 0.5 \text{ cm}$  and z-coordinate of the track vertex  $|z| < 12 \text{ cm}$
  - Quality of track reconstruction in the  $r - \phi$  and z-planes  $\chi^2 < 30$
  - Track ionization losses  $dE/dx$  in the drift chamber:

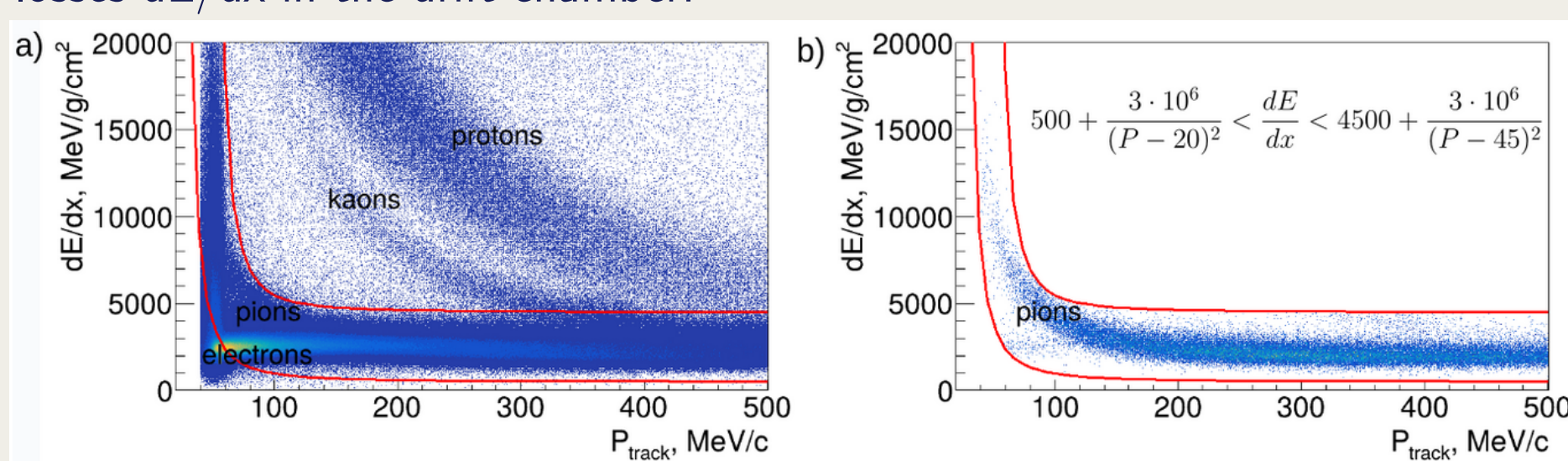


Figure 3. Ionization losses in a drift chamber as a function of track momentum in experiment and simulation.

- **Good photons**  $\eta \rightarrow \gamma\gamma$ ,  $\pi^0 \rightarrow \gamma\gamma$ 
  - $3 < \text{number of photons} < 10$
  - photon energy  $> 30 \text{ MeV}$ , partially suppresses background from processes with low-energy photons
  - beam energy greater than 120 MeV, exceeding the photon energy
  - photons from BGO at small angles with energies  $< 60 \text{ MeV}$  are excluded
- **Total momentum and energy**  $\Delta E = \Sigma E - 2E_{beam} < 150$ ;  $\Sigma P < 150$

## Kinematic reconstruction

For the selected events, a kinematic reconstruction procedure[\*] is performed in the 5C hypothesis:

- The coordinates of the vertex in the transverse plane are fixed, and the z-coordinate is sought.
- The sum of the particle momenta is zero.
- The particle energy is equal to twice the beam energy.
- $\pi^0$  mass constrain. The four photons with the smallest  $\chi^2$  are selected.

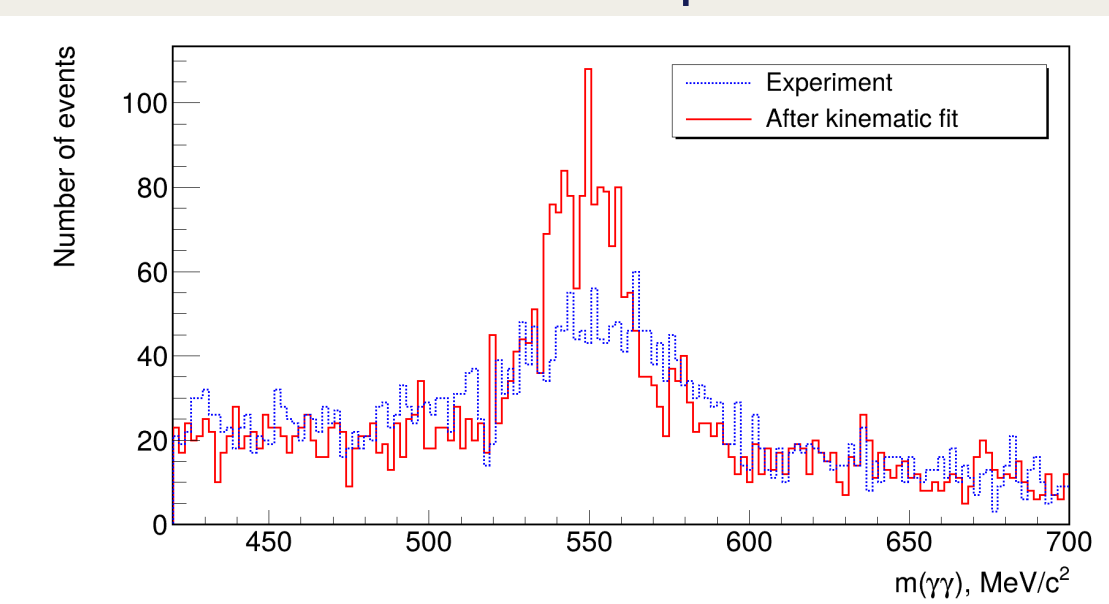


Figure 4. Signal from the  $\eta$ -meson at the point with  $E_{c.m.} = 1600 \text{ MeV}$  before reconstruction (dashed line) and after (solid line)

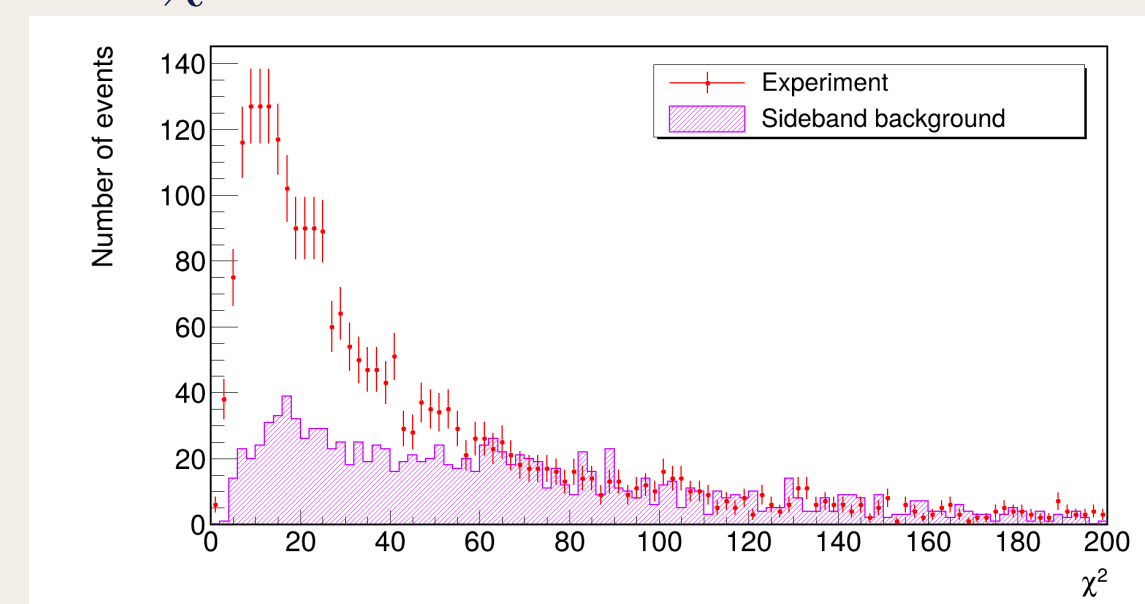


Figure 5. Distribution  $\chi^2$  for signal (mass of  $\eta \in (500; 600) \text{ MeV}$ ) and background (mass of  $\eta \in (450; 500) \cup (600; 650) \text{ MeV}$ ) regions

[\*] Gribanov S.S., Popov A.S. Kinematic and vertex fitting package for the CMD-3 experiment // arXiv:2208.11569v7

## Fit functions

The resonances were fitted by convolution of a Gaussian with a Breit-Wigner:

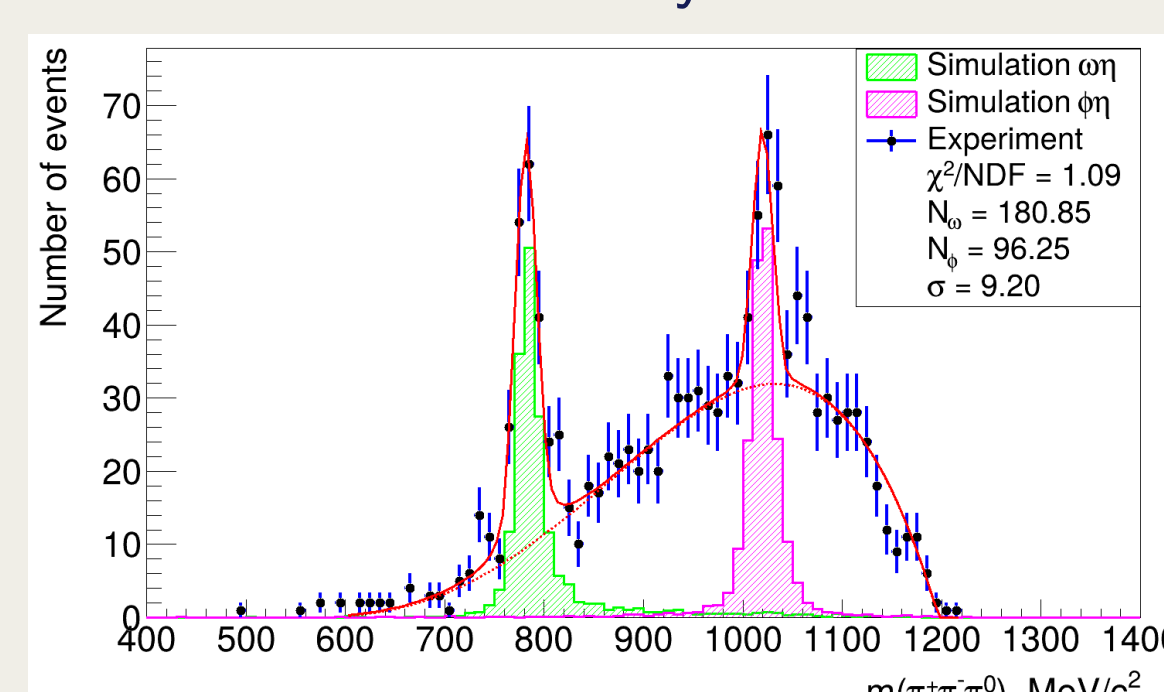


Figure 6. The  $\pi^+\pi^-\pi^0$  invariant mass distribution. Histograms show expected MC-simulated signals from the  $\omega(782)\eta$  and  $\phi(1020)\eta$  intermediate states.

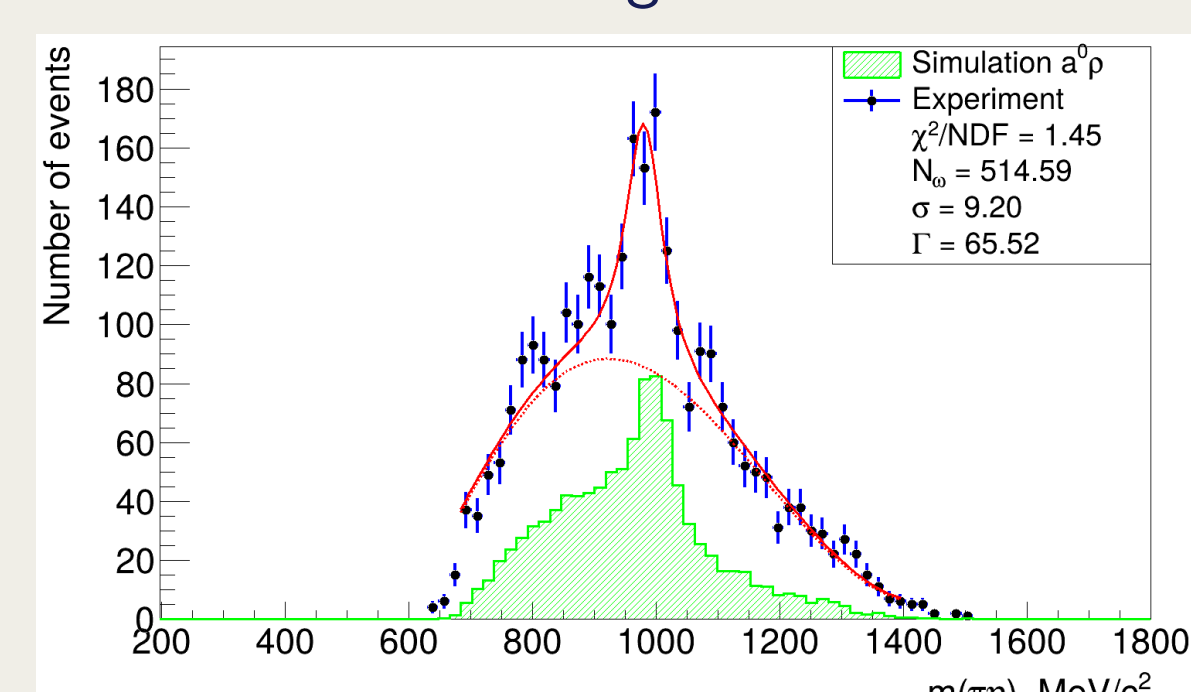


Figure 7. The  $\pi\eta$  invariant mass distribution. Histogram shows expected MC-simulated signal from the  $a_0(980)\rho(770)$  intermediate state.

## Detection efficiency

To determine the detection efficiency, a simulation of  $N_0 = 50,000$  events for three intermediate states  $\omega(782)\eta$ ,  $\phi(1020)\eta$  and  $a_0(980)\rho(770)$  was used.

$$\epsilon = N/N_0, \Delta\epsilon = \sqrt{\epsilon(1-\epsilon)/N_0}$$

The efficiency for  $e^+e^- \rightarrow \pi^+\pi^-\pi^0\eta$  was calculated as a weighted average of the efficiencies of these states, where the weights corresponded to the numbers of events observed in the experiment:  $\bar{\epsilon} = \Sigma N_i \epsilon_i / \Sigma N_i$

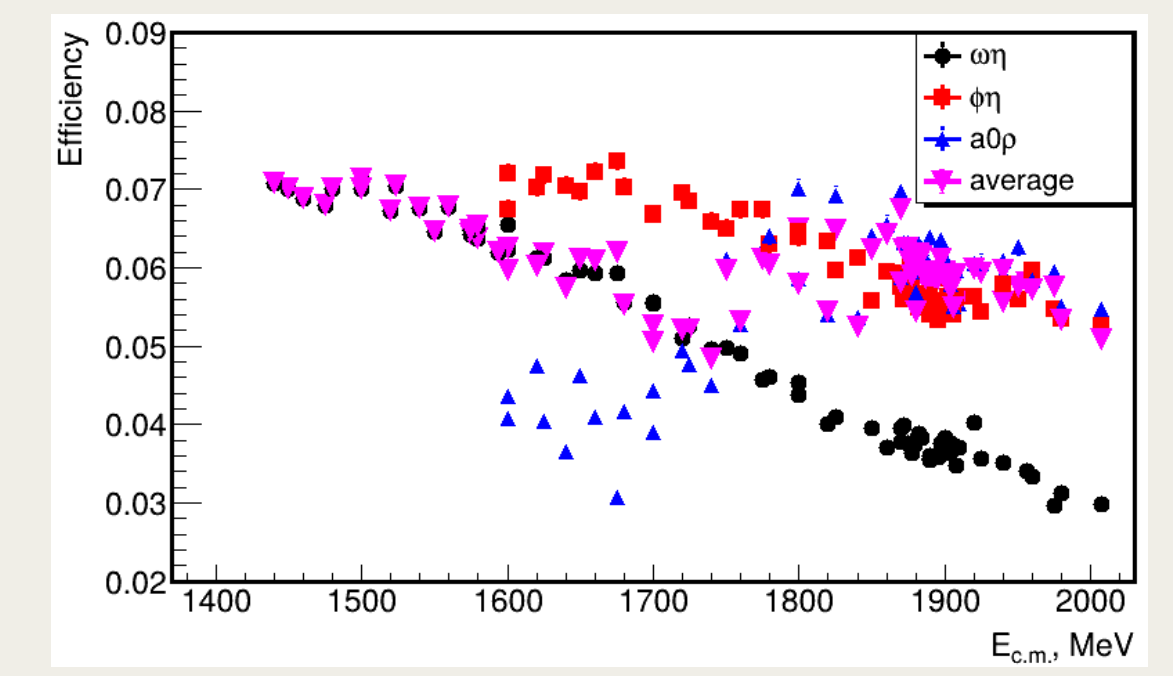


Figure 8. The detection efficiency depending on the energy in the c.m.

## Radiative correction

The radiative correction is calculated iteratively using the formula:

$$\sigma_{vis} = \int_0^{\Delta E/E} \sigma_{born}(s(1-x))F(x,s)dx,$$

where  $\sigma_{vis} = \sigma_{born}(1 + \delta_R)$

Initial approximation:  $\sigma_{vis} = N_{data}/(L\epsilon)$

The cross section is fitted in a two-resonance model.

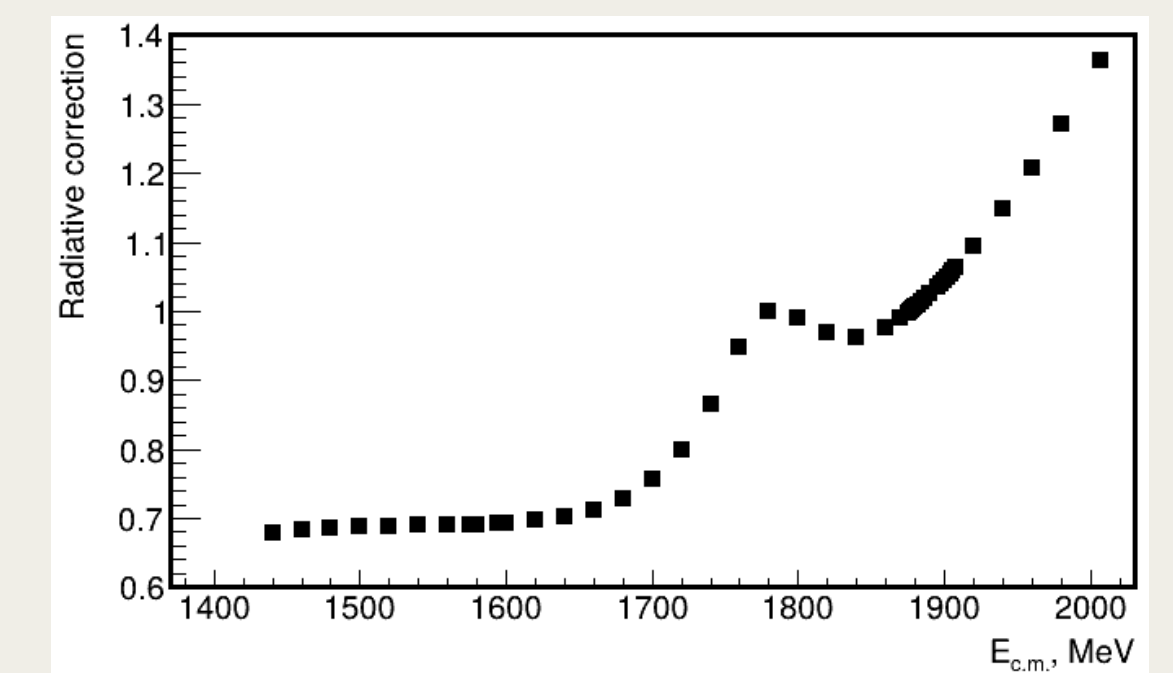


Figure 9. The radiation correction depending on the energy in the c.m.

## Correction to the registration efficiency

To determine the discrepancy in the registration efficiency of neutral particles  $\eta$  and  $\pi^0$  in experiment and simulation, a kinematic fit was made in the 2C hypothesis of lost  $\pi^0$  and the correction was calculated as follows:

$$\frac{N_{events\ with\ \pi^0}(MC)}{N_{all\ events}} \cdot \frac{N_{events\ with\ \pi^0}(Exp)}{N_{all\ events}} = 1.05 \pm 0.02$$

The correction for charged pions was studied with the 3C hypothesis of lost  $\pi^\pm$ , calculated similarly and amounted to  $0.99 \pm 0.05$

The values shown are averaged over all energy points.

## Cross sections

The Born cross section:

$$\sigma_{born} = \frac{N_{data}}{L\epsilon(1+\delta_R)(1+\delta_\epsilon)}$$

, where  $N_{data}$  - number of signal events,  $L$  - integral luminosity,  $\epsilon$  - registration efficiency,  $(1 + \delta_R)$  - radiation correction,  $(1 + \delta_\epsilon)$  - correction to the registration efficiency.

**Systematic uncertainty:** luminosity 1%, radiative correction 1%, correction for the detection efficiency of charged 9% and neutral 4% particles, selection criteria variation 1%. The quadratic sum — 10%.

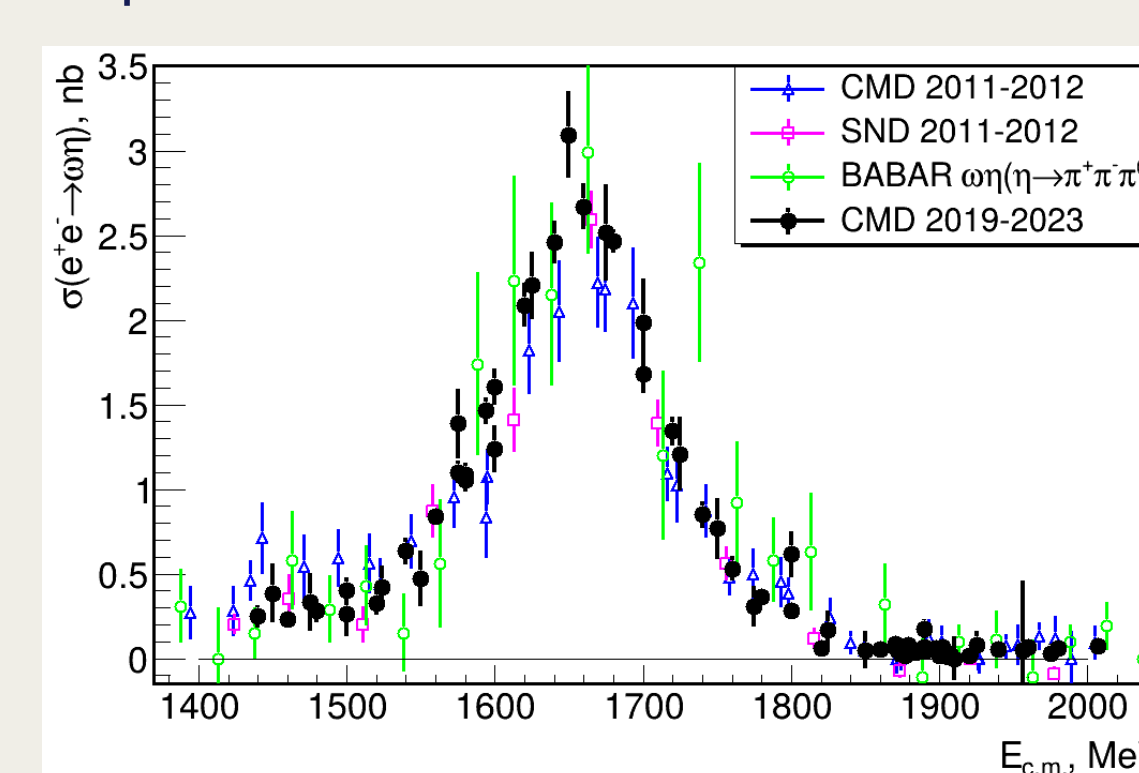


Figure 10. The cross section of the process  $e^+e^- \rightarrow \omega(782)\eta$

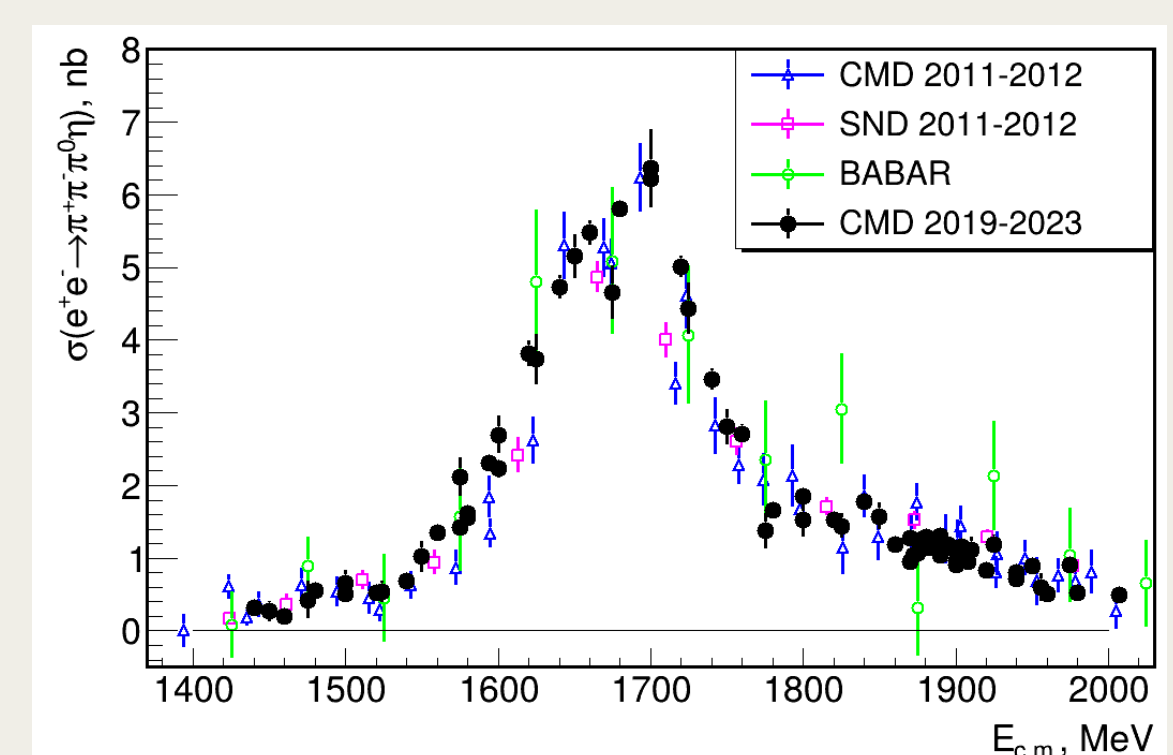


Figure 12. The cross section of the process  $e^+e^- \rightarrow \pi^+\pi^-\pi^0\eta$

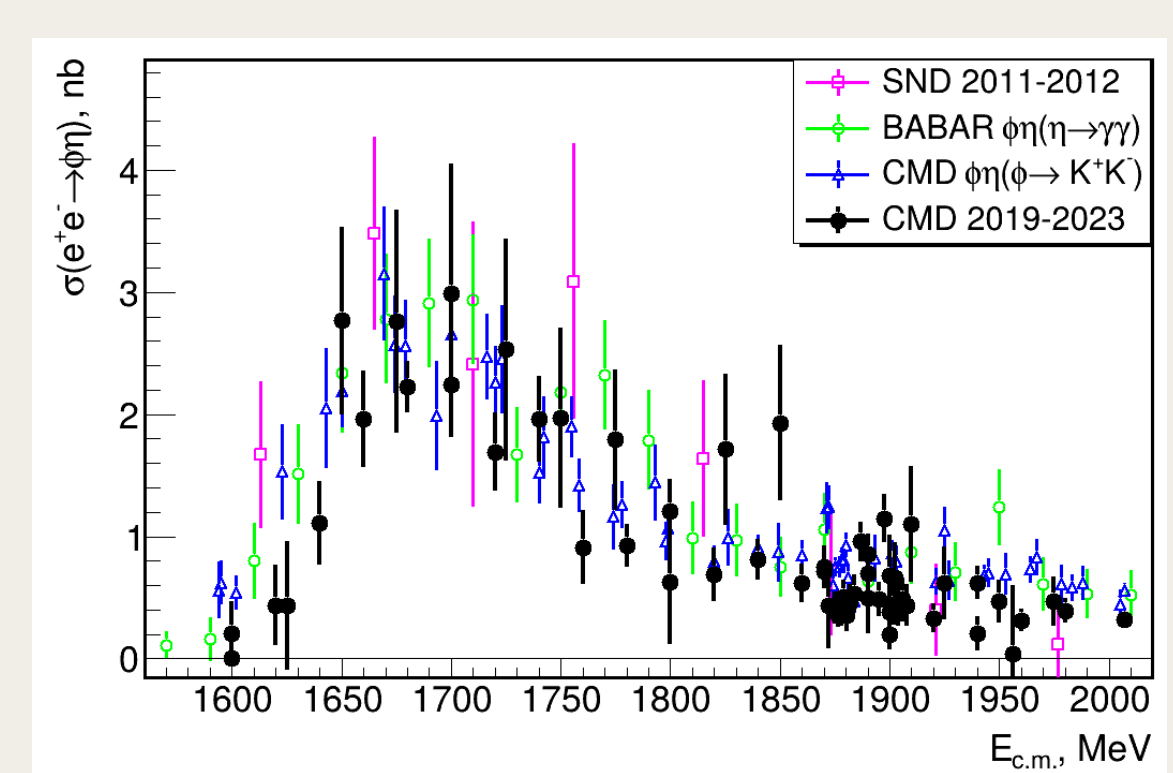


Figure 13. The cross section of the process  $e^+e^- \rightarrow \phi(1020)\eta$

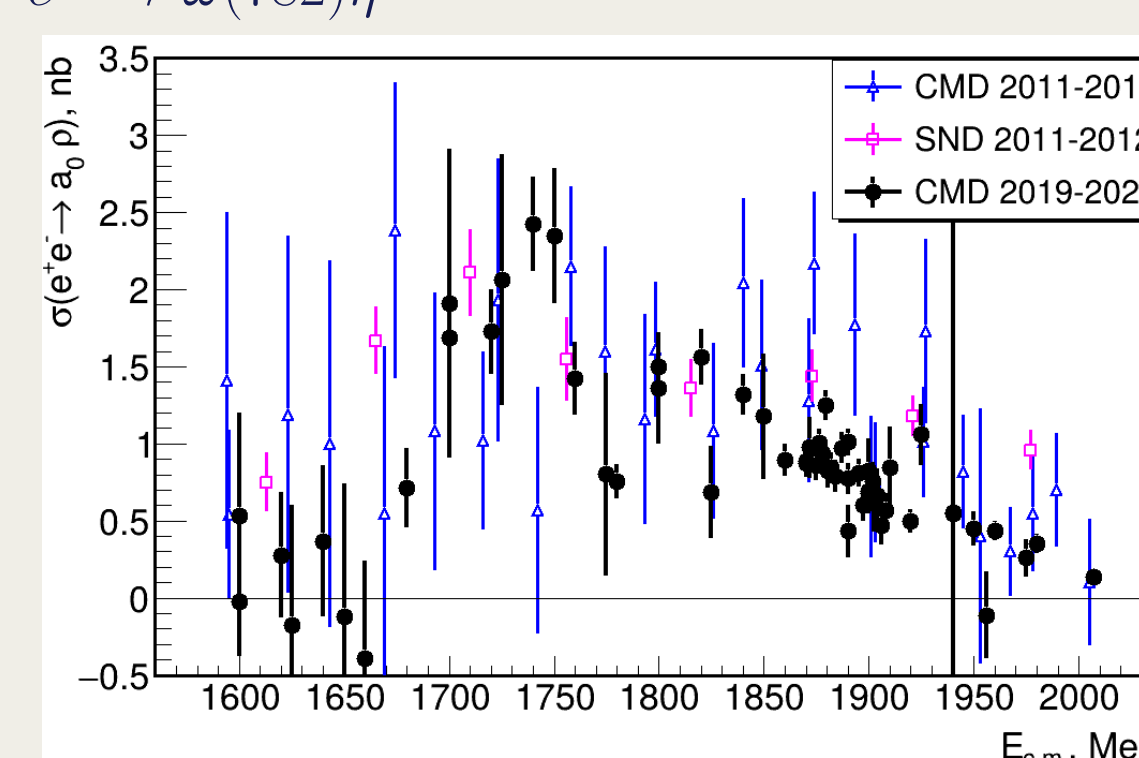


Figure 11. The cross section of the process  $e^+e^- \rightarrow a_0(980)\rho(770)$

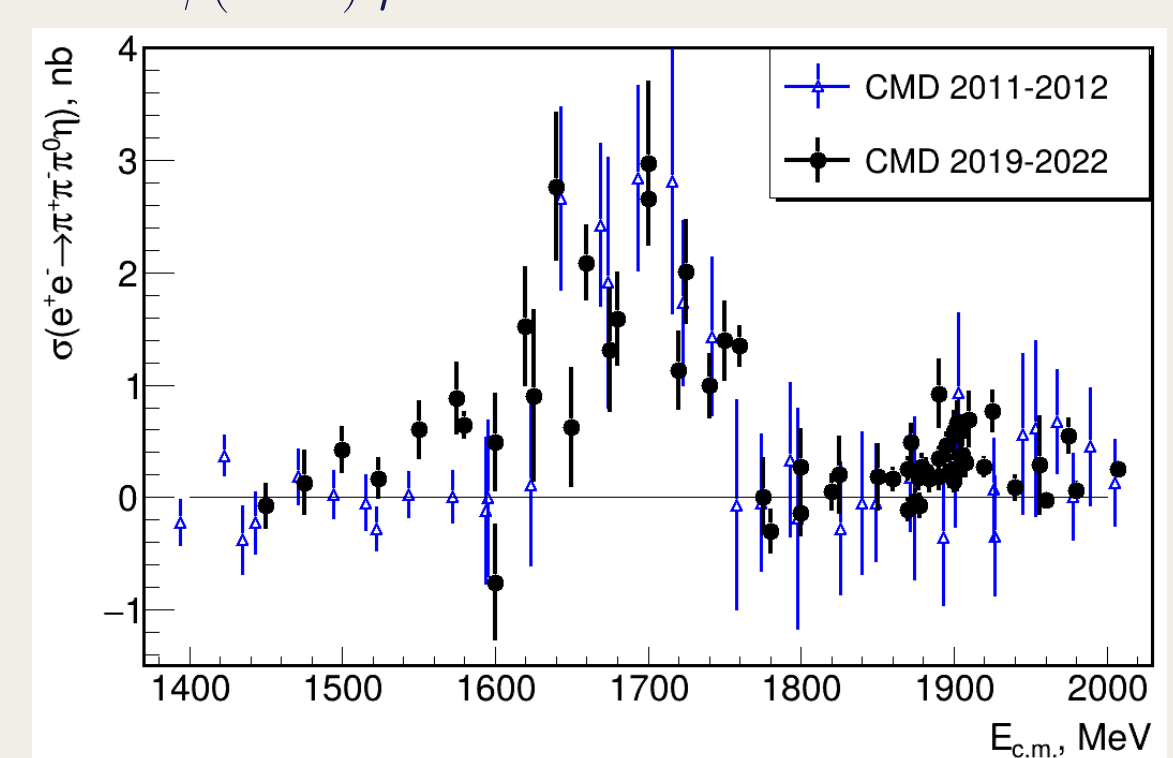


Figure 14. The cross section of the process  $e^+e^- \rightarrow \pi^+\pi^-\pi^0\eta$  ( $no\ \omega, \phi, a_0$ )

## Future plan

Study the dynamics of the process for the presence of contributions from unaccounted intermediate resonances, investigate the interference between resonances.